Density of states in layered superconductor-insulator structures

Branko P. Stojković* and Oriol T. Valls
School of Physics and Astronomy, University of Minnesota, Minneapolis, Minnesota 55455-0149
(Received 7 September 1994)

We study superconductor-insulator layered structures, using a microscopic method based on the Gor'kov equations. We present our results for the single-particle density of states and the order parameter (OP) as a function of the experimental parameters, such as the insulating barrier strength, the coherence length, and the range of transverse momentum of probes. The results provide a very good fit to the tunneling spectra of $Bi_2Sr_2CaCu_2O_8$, obtained in a soft-point-contact scanning-tunneling microscopy measurement. The results also indicate that the OP in strongly coupled superconducting regions (such as CuO planes in high-temperature superconductors), may be significantly larger than the energy gap found in experiments. The role of all relevant physical and geometrical parameters is also discussed.

I. INTRODUCTION

Most of the several classes of high-temperature superconductors (HTSC's) exhibit a characteristic inhomogeneous, layered structure. The role of this structure and the function of the various layers in it are still not well understood. Most models of high-temperature superconductivity assume that these materials are essentially two dimensional and in general that superconductivity originates in certain oxide layers, separated by nonsuperconducting regions. For many purposes[1] the coupling between neighboring superconducting layers is assumed to be negligible. However, it has been argued in the context of other models[2] that this coupling can be extremely important, and perhaps crucial for an understanding of the mechanism of high-temperature superconductivity.

HTSC's are customarily classified into "families" depending on the degree of anisotropy present. In Ref. 3 we studied a model for the case where the separation between strongly superconducting oxide layers is not very large and the intervening layers can be considered normal metallic. We showed that good agreement with experimental tunneling results for $Nd_{2-x}Ce_xCuO_{4-y}$ can be obtained from that model. On the other hand, several experiments[4] have reported, in the most inhomogeneous cases such as the $Bi_2Sr_2CaCu_2O_8$ (BSCCO) family, the observation of "Shapiro steps," which is an indication that there are actually insulating layers between the superconducting regions. The existence of these layers can dramatically affect, e.g., scanning-tunneling microscopy (STM) measurements, since the insulating layers would allow multiple quasiparticle reflections, and therefore create the complicated structure which has been observed in the density of states (DOS).[5]

Prior to the discovery of HTSC's, layered superconductor-insulator (SI) structures had been theoretically studied mostly in the context of the phenomenological Lawrence-Doniach[6] model, or microscopically in the context of chemically anisotropic samples. The large anisotropy of HTSC's and their short coherence length[7] have in practice excluded the applicability of any phenomenological theory to the tunneling experiments performed on these materials. Microscopically, the tunneling spectra of BSCCO have been modeled by considering the unit cell as a stack of coupled metallic layers with different superconducting coupling strengths.[2,8] However, these models have a relatively large number of fitting parameters, some of which cannot be estimated from the existing experimental data. Moreover, the existence of the finite-thickness insulating layer has not yet been taken into account in calculations of the tunneling spectra, and in some of the above models the order parameter is assumed constant in each layer, and it is not determined self-consistently.

In this paper we develop a microscopic self-consistent theory for short coherence length superconductor-insulator atomic-scale structures. We present results for both the superconducting order parameter (OP) and the tunneling DOS. Just as in Ref. 3, the method used is based on the self-consistent solution of the Gor'kov equations, considered in the appropriate geometry. Here the results are presented as a function of the coherence length, layer thicknesses, insulator barrier height, and the range of transverse momentum of the probe, which has to be taken into account. We study the influence of these physical parameters on our results. We compare our results for the DOS with tunneling data obtained in a soft-point-contact STM measurement, performed on BSCCO,[5] by making a number of physical assumptions. In our discussion, we assume that pairing in BSCCO is in a conventional s-wave state. This issue is currently controversial in high-temperature superconductors,[9] and is further briefly addressed in the conclusions. We examine how the surface quality in experiments can alter their outcome and show how identical quasiparticle spectral functions can produce different measured DOS.

The results given here can be summarized as follows: We find that our calculated results for the tunneling spectra in SI-layered compounds, obtained using reasonable values of the input and fitting parameters, are in good agreement with the experimental data[5] obtained for BSCCO. We attribute the characteristic structure observed in these experiments to interference phenomena occurring because of the insulating barriers. We show

0163-1829/95/51(5)/3186(9)/$06.00

why one obtains different peaks in the DOS, depending on the contact position. In comparison to non-self-consistent models, we find that our self-consistent results differ in that the peak structure is substantially shifted. Our calculation always shows a clear gaplike structure in the DOS, which was often impossible to obtain within non-self-consistent approaches.

This paper is organized as follows: In Sec. II we review the theoretical model for our self-consistent calculations. Section III contains the results, their analysis for many different values of physical parameters, and the comparison with experiment. Finally, in Sec. IV we summarize our conclusions and discuss the implications and limitations of our results.

II. MODEL

In this section we present the model used to self-consistently calculate the OP and the tunneling DOS for a superconductor-insulator-layered system. We consider a layered structure, consisting of an infinite series of superconducting and insulating slabs, i.e., an infinite system uniform in the x, y directions and with alternating S and I layers, each of thickness d_S and d_I, respectively, stacked along the z direction.

Our starting point is the Gor'kov equations for a superconductor in an "external" potential U, which here accounts for the presence of insulating layers. In the chosen geometry the potential $U(\mathbf{r})$ is effectively only a function of z, i.e., $U(\mathbf{r}) \equiv U(z)$. It has a large value in the insulating layers and is zero in the superconducting layers. We assume that the fermions interact through a point-contact attractive interaction of unspecified origin, acting between fermions within an energy range ω_0 from the Fermi surface. In zero applied field, and in the system of units where $\hbar = k_B = 1$, these equations can be written as[10]

$$\left[i\omega_n + \frac{\nabla_\perp^2}{2m_{ab}} + \frac{\nabla_z^2}{2m_c} + \mu - U(\mathbf{r})\right] G(\mathbf{r},\mathbf{r}',\omega_n) + \Delta(\mathbf{r})\, F^\dagger(\mathbf{r},\mathbf{r}',\omega_n) = \delta(\mathbf{r}-\mathbf{r}'), \tag{2.1a}$$

$$\left[-i\omega_n + \frac{\nabla_\perp^2}{2m_{ab}} + \frac{\nabla_z^2}{2m_c} + \mu - U(\mathbf{r})\right] F^\dagger(\mathbf{r},\mathbf{r}',\omega_n) = \Delta^*(\mathbf{r})\, G(\mathbf{r},\mathbf{r}',\omega_n)\ , \tag{2.1b}$$

where G and F are the normal and anomalous Green's functions, respectively, m_c and m_{ab} are the effective masses, and ∇_z and $\nabla_\perp$ the gradients for motion along the c axis and in the ab plane, respectively. We assume that the chemical potential μ is equal to the Fermi energy E_F, which belongs to a single energy band.

Since the system considered is isotropic in the x-y directions, it is convenient to perform a spatial Fourier transform in the ab plane. Thus, Eqs. (2.1) become

$$\left[i\omega_n + \frac{\nabla_z^2}{2m_c} + \mu_z - U(z)\right] G(z,z',k_\perp,\omega_n) + \Delta(z)\, F^\dagger(z,z',k_\perp,\omega_n) = \delta(z-z'), \tag{2.2a}$$

$$\left[-i\omega_n + \frac{\nabla_z^2}{2m_c} + \mu_z - U(z)\right] F^\dagger(z,z',k_\perp,\omega_n) = \Delta^*(z)\, G(z,z',k_\perp,\omega_n), \tag{2.2b}$$

where

$$\mu_z = \mu - \frac{k_\perp^2}{2m_{ab}} \equiv \mu - \epsilon(k_\perp), \tag{2.3}$$

and $\mathbf{k}_\perp$ is the wave vector in the transverse direction, $\mathbf{k}_\perp \equiv (k_x, k_y)$. We will be considering an infinite "lattice," with periodic boundary conditions. Therefore U can be written as

$$U(z) = \sum_{m=-\infty}^{\infty} v(z - dm), \tag{2.4}$$

where v is a "single-layer" potential and $d = d_S + d_I$ is the lattice constant. Equations (2.2) must be solved together with the self-consistency equation

$$\Delta^*(z) = g(z) T \sum_n \int \frac{d^2k_\perp}{(2\pi)^2} F^\dagger(z,z,k_\perp,\omega_n), \tag{2.5}$$

where $g(z)$ is the spatially dependent superconducting coupling.

In general, the system of equations (2.2) and (2.5) is hard to solve. On the other hand, it is relatively easy, and as we shall see, very reasonable, to consider a system of noninteracting fermions in the periodic "external" potential U in the tight-binding approximation. One begins by solving the eigenvalue problem

$$\left[-\frac{\nabla_z^2}{2m_c} + U(z)\right] \Psi_\nu(k_z,z) = E_\nu(k_z)\, \Psi_\nu(k_z,z)\ , \tag{2.6}$$

where $E_\nu(k_z)$ is the eigenvalue as specified in terms of the quantum numbers k_z and ν. The latter may be viewed as a "subband" index of the energy band we consider. $\Psi_\nu(k_z,z)$ is a Bloch function, and k_z is the wave vector of a Bloch particle in the z direction. Provided that the S layers are sufficiently separated (i.e., the barrier sufficiently strong), one can seek the solution of Eq. (2.6) in the tight-binding approximation. $\Psi_\nu(k_z,z)$ can be written as

$$\Psi_\nu(k_z,z) = \frac{1}{N^{1/2}} \sum_m \varphi_\nu(z - dm)\, \exp(imk_z d)\ , \tag{2.7}$$

where N is the number of superconducting (insulating) layers, and φ_ν satisfies

$$\left[-\frac{\nabla_z^2}{2m_c}+v(z)\right]\varphi_\nu(z)=\varepsilon_\nu\,\varphi_\nu(z). \tag{2.8}$$

In the tight-binding approximation one then has

$$E_\nu(k_z)\approx\varepsilon_\nu+B_\nu+2A_\nu\cos(k_z d), \tag{2.9}$$

where

$$A_\nu=\int dz\,\varphi_\nu^*(z)\,[U(z)-v(z)]\,\varphi_\nu(z-d)\ , \tag{2.10a}$$

$$B_\nu=\int dz\,\varphi_\nu^*(z)\,[U(z)-v(z)]\,\varphi_\nu(z). \tag{2.10b}$$

The quantities A_ν and B_ν are referred to as the subband width and the subband shift, respectively. To complete the solution of the model we have to specify explicitly the potential $v(z)$. Within the tight-binding approximation, the validity of which we further discuss below, the exact form of the barrier is unimportant, since the quantities (2.10) are all that is required. For simplicity, we will consider here a square barrier for the insulating layer (as in the Kronig-Penney model). Thus, we assume that $v=0$ (bottom of the band) in the superconducting layer and $v=V_0>E_F$ in the insulating region. For this model, it is an elementary matter to obtain analytic expressions for φ_ν and numerical values for ε_ν.

It is convenient to expand the Green's functions G and $F^\dagger$, in terms of the complete set of Bloch functions $\Psi_\nu(k,z)$, defined in Eq. (2.7):

$$G(z,z',k_\perp,\omega_n)\equiv\sum_{\nu,\nu',k_z}\Psi_\nu(k_z,z)\,\Psi_{\nu'}^*(k_z,z')\,g_{\nu,\nu'}^{k_z}(k_\perp,\omega_n), \tag{2.11a}$$

$$F^\dagger(z,z',k_\perp,\omega_n)\equiv\sum_{\nu,\nu',k_z}\Psi_\nu(k_z,z)\,\Psi_{\nu'}^*(k_z,z')\,f_{\nu,\nu'}^{k_z}(k_\perp,\omega_n). \tag{2.11b}$$

In Eqs. (2.11), the Bloch functions have the same index k_z, which is a consequence of the tight-binding approximation and the periodic boundary conditions used. The sum over subband indices is limited by the condition that the relevant energies $\epsilon(k_\perp)+E_\nu(k_z)$ be within a range of order ω_0 from the Fermi surface.[3] In the absence of applied fields the mean field order parameter has a constant phase throughout a single superconducting layer, but the phases in two neighboring layers may be different. For simplicity, we shall assume that the OP phase is constant throughout the whole sample, although it is relatively easy to include a varying phase in the formalism. We then write

$$\Delta(z)=\sum_{\nu,k_z}\Psi_\nu(k_z,z)\,\Delta_\nu(k_z)\ . \tag{2.12}$$

One easily verifies that in the tight-binding approximation only $\Delta_\nu(k_z=0)\equiv\Delta_\nu$ is nonvanishing. Then, using the orthogonality of the Bloch functions, the Gor'kov equations (2.2) become

$$[i\omega_n-E_\nu(k_z)+\mu_z]\,g_{\nu,\nu'}^{k_z}+\sum_{n''}C_{\nu,\nu''}f_{\nu'',\nu'}^{k_z}=\delta_{\nu,\nu'}\ , \tag{2.13a}$$

$$[-i\omega_n-E_\nu(k_z)+\mu_z]\,f_{\nu,\nu'}^{k_z}=\sum_{\nu''}C_{\nu,\nu''}g_{\nu'',\nu'}^{k_z}, \tag{2.13b}$$

where we have introduced the matrix $\underline{C}$, with matrix elements

$$C_{\nu,\nu'}=\frac{1}{N^{1/2}}\sum_{\nu''}\Delta_{\nu''}\int dz\,\varphi_\nu(z)\varphi_{\nu'}(z)\varphi_{\nu''}(z). \tag{2.14}$$

As in previous work,[3] one can define matrices $\underline{G}$, $\underline{F}$, and $\underline{X}$, with matrix elements

$$G_{\nu,\nu'}\equiv g_{\nu,\nu'}^{k_z}(k_\perp,\omega_n),\qquad F_{\nu,\nu'}\equiv f_{\nu,\nu'}^{k_z}(k_\perp,\omega_n),$$

$$X_{\nu,\nu'}\equiv[E_\nu(k_z)-\mu_z]\,\delta_{\nu,\nu'}, \tag{2.15}$$

and transform the Gor'kov equations (2.13) into a set of matrix equations, with a formal solution

$$\underline{F}=\left[\underline{C}-(i\omega_n-\underline{X})\,\frac{1}{\underline{C}}\,(i\omega_n+\underline{X})\right]^{-1} \tag{2.16}$$

and

$$\underline{G}=-\frac{1}{\underline{C}}\,(i\omega_n+X)\,\underline{F}. \tag{2.17}$$

Defining an effective coupling tensor Λ,[3]

$$\Lambda_{\nu,\nu',\nu''}=\frac{1}{N^{1/2}}\int dz\,g(z)\,\varphi_\nu(z)\,\varphi_{\nu'}(z)\,\varphi_{\nu''}(z), \tag{2.18}$$

the self-consistency equation (2.5) transforms into

$$\Delta_\nu=T\sum_{\nu',\nu'',k_z}\Lambda_{\nu,\nu',\nu''}\int\frac{d^2k_\perp}{(2\pi)^2}\sum_{\omega_n}F_{\nu',\nu''}\ . \tag{2.19}$$

Equations (2.19), (2.16), and (2.17) are the central equations of this paper. In general, they are solved numerically. Self-consistency is obtained using an iteration procedure, similar to those used in Ref. 3. The procedure is stopped when the maximum relative change in $\Delta(z)$ $(0<z<d)$, between two successive iterations, is less than 1×10^{-4}.

Once the OP is obtained self-consistently, one can perform the analytic continuation for G, i.e., $G(z,z',k_\perp,i\omega_n)\to G(z,z',k_\perp,E)$, and then calculate the spectral density:

$$N(z,k_\perp,E) = -\frac{1}{\pi}\,\mathrm{Im}\,G(z,z,k_\perp,E+i\tau) \qquad (2.20)$$

(where τ is a small positive quantity). The DOS can then be found by integrating $N(z,k_\perp,E)$ over the appropriate ranges of $\mathbf{k}_\perp$ and z.

It is important to discuss the range of validity of the tight-binding approximation used here. In general, this approximation is applicable when the widths A_ν and the shifts B_ν, defined in Eq. (2.10), are small compared to the separation of the energy subbands. In other words, both A_ν and B_ν must be small compared to $\Delta\varepsilon \sim |\varepsilon_\nu - \varepsilon_{\nu\pm1}|$, for all relevant ν. As discussed in Ref. 11, a typical measure of $\Delta\varepsilon$, in the absence of mass anisotropy ($m_{ab} = m_c$), is of order $E_F\,(k_F d_S)^{-1}$, while Eq. (2.10a) yields $A_\nu \sim V_0 \exp(-\kappa k_F d)$, where $\kappa \sim \sqrt{V_0/E_F - 1}$. Therefore, the approximation is valid if

$$\frac{1}{k_F d_S} \gg \frac{V_0}{E_F}\exp(-\kappa k_F d). \qquad (2.21)$$

Assuming that $V_0 - E_F$ is comparable to E_F, which is the case in the experimental situations of interest in this paper, we have that $\kappa \sim 1$ and condition (2.21) becomes

$$\frac{1}{k_F d_S} \gg \exp(-k_F\, d)\ , \qquad (2.22)$$

which is easily satisfied for $k_F d_I$ and $k_F d_S$ larger than, or of order unity. For systems with mass anisotropy, where $m_{ab} \neq m_c$, Eq. (2.22) becomes

$$\frac{1}{k_F d_M}\,\frac{m_{ab}}{m_c} \gg \exp\left(-k_F\, d\sqrt{\frac{m_c}{m_{ab}}}\right)\ , \qquad (2.23)$$

which means that when $m_c \gg m_{ab}$, which is the case in HTSC's, the tight-binding approximation is even more favorable.

III. RESULTS

In this section we discuss results obtained from the methods presented in Sec. II. We study both the OP and the DOS in the experimentally relevant cases where d_I is small. Results are presented for several values of the coherence length, thicknesses (geometry), and the ranges of integration of Eq. (2.20), in order to study the variation of the results with these parameters. The results presented are mostly computed in the low-temperature limit, $T \to 0$, and should be valid at $T \ll T_c$. Finally, we compare our results to the tunneling spectra obtained experimentally[5] in the anisotropic cuprate BSCCO. We explain how the input parameters for the theory are inferred from experiments through the use of a number of physical assumptions and show that our theoretical results quantitatively fit the observed experimental data.

There are several physical parameters in our model,[3,11,12] but only some of their dimensionless ratios are relevant, since several of the parameters are simply related to each other. We choose a parametrization similar to that used in previous work.[3,11–13] The input parameters are $k_F\xi_0$, Δ_0^S/ω_0, and V_0/E_F. Note that Δ_0^S is the order parameter at $T = 0$ for bulk S material, i.e., a hypothetical infinite (in all directions) S material. In addition, we specify the geometry by $k_F d_S$, and $k_F d_I$. For the function $g(z)$ we simply take a constant g_S, easily related to Δ_0^S/ω_0, except, as indicated, in the comparison with experiment. Similarly, we take the mass anisotropy into account in the comparison with experiment, but the other results quoted are obtained using an isotropic effective mass, $m_{ab} = m_c$.

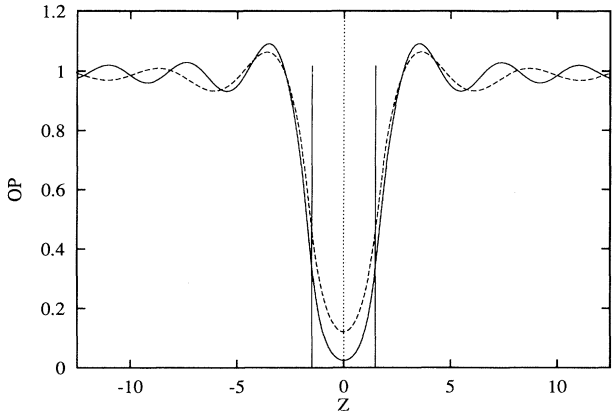

FIG. 1. The normalized OP vs $Z \equiv k_F z$, across a thin insulating barrier, $k_F d_I = 3$, between two thicker superconducting layers, $k_F d_S = 55$, $\pi k_F \xi_0 = 20$. The solid and dashed lines show the cases when the barrier height is $V_0 = 3\,E_F$ and $V_0 = 1.5\,E_F$, respectively. The vertical lines mark the SI interfaces.

We first study the particular relevance of the input parameters and the relative sensitivity of our results to their assumed values. At the same time, we further justify the tight-binding approximation used here. We begin by showing how the OP extends through the insulating region between two superconducting layers, depending on the barrier height (Fig. 1). Since we assume periodic boundary conditions in this work, we do not display more than one "cell" in our plots of $\Delta(z)$. The physical parameters are $k_F d_S = 55$, $k_F d_I = 3$. The coherence length is assumed short, $\pi k_F \xi_0 = 20$, and we take $\Delta_0^S/\omega_0 = 0.5$. The solid line shows the case where $V_0/E_F = 3$, and the dashed line that where $V_0/E_F = 1.5$. Obviously, in both cases, the OP extends throughout the insulator only marginally, thus proving that, when $V_0 - E_F$ is comparable to E_F, the results are not strongly dependent on V_0 and the validity of the tight-binding approximation is indeed justified [see Eqs. (2.21) and (2.22)]. Moreover, since the OP here is calculated using the expansion (2.12), the fact that $\Delta(z)$ in the I layer assumes a value much smaller than that in the S layer indicates that the wave functions obtained from Eq. (2.8) are indeed well localized and therefore the Bloch functions we use are a correct complete set of functions for the systems we study.

Next, we show how the barrier thickness affects the above considerations. Figure 2 shows the same quantity as that plotted in Fig. 1: The solid line is identical to that in Fig. 1, while the dashed line corresponds to the same

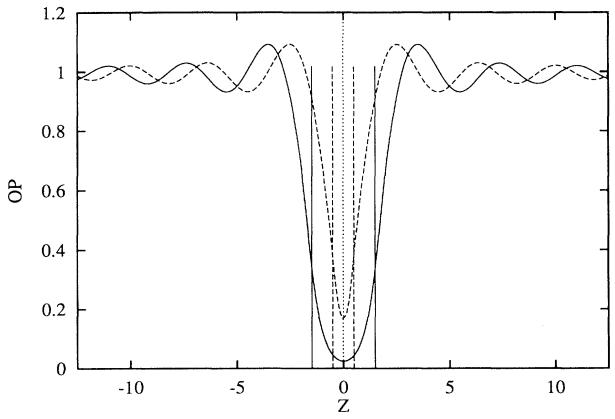

FIG. 2. As in Fig. 1, but for two thin insulating barriers, $k_F d_I = 3$ (solid line) and $k_F d_I = 1$ (dashed line). For both curves $V_0 = 3\,E_F$.

parameter values as the solid one, except for a lower value of the I-layer thickness, $k_F d_I = 1$. Both quantities are normalized with respect to Δ_S^0. Clearly, the OP assumes a much higher value in the I layer in the latter case, but the value of the OP is still much lower than in the S layers and the tight-binding approximation is still valid. This is again in agreement with the discussion of Eq. (2.22).

We now turn to the local DOS, which is the main quantity of interest. Figure 3 shows the DOS for the two systems depicted in Fig. 1, as would be seen in a tunneling experiment: The quantity plotted, defined in Eq. (2.20), is averaged over a range of z equal to ξ_0, starting from the metal-insulator interface. The range of $k_\perp$ integration is small, $|k_\perp| < k_\perp^{\max} = 0.04\,k_F$. In this and the following three figures the energy is given in units of Δ_0^S. The solid (dashed) line here corresponds to the system displayed by a solid (dashed) line in Fig. 1. The choices of z and $k_\perp^{\max}$ ranges are motivated by experiment: The outermost layer in a real, finite size sample is insulating, and assuming that the OP in the S layers is not very affected by the surface, tunneling probes the sample only to within $z \sim \xi_0$ from the first S-I interface.

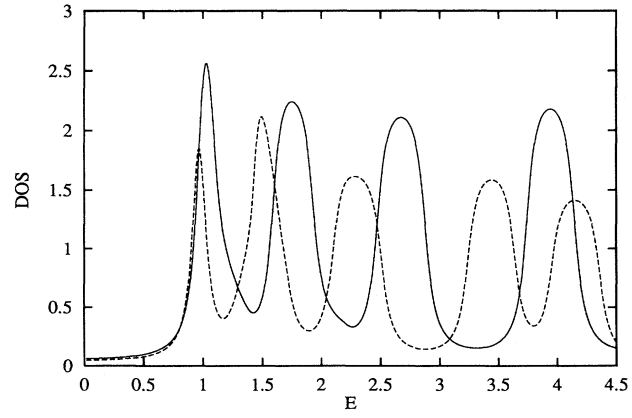

FIG. 3. Local DOS for systems depicted in Fig. 1. E is in units of Δ_0^S, and the DOS is normalized with respect to its normal-metal limit. The solid (dashed) line corresponds to the system shown by a solid (dashed) line in Fig. 1.

The choice of $k_\perp^{\max}$ range is justified from the following argument: We consider particles of energy E arriving at a tunneling barrier of thickness δ, and we assume that their motion is not strongly affected by the local electric field (which is the case in many planar or soft-contact measurements).[14] Then, one can easily estimate the probability p for the tunneling of particles with small transverse momentum $k_\perp$:

$$p \sim p_0 \exp\left(-\frac{\epsilon_\perp \delta}{2}\sqrt{\frac{2m}{V-E}}\right), \tag{3.1}$$

where p_0 is the tunneling probability for particles with $k_\perp = 0$, $\epsilon_\perp = k_\perp^2/2m_{ab}$, and V is the barrier height. Assuming that $V - E$ is comparable to the Fermi energy, it is readily seen that the calculation of tunneling spectra should take into account particles with $k_\perp$ given by the range ($m_c = m_{ab}$):

$$k_F \delta \left(\frac{k_\perp^{\max}}{k_F}\right)^2 \sim 1. \tag{3.2}$$

Including the mass anisotropy in the above argument, the maximum $k_\perp$ should be of order

$$k_\perp^{\max} \sim \left[\frac{1}{k_F \delta}\left(\frac{m_{ab}}{m_c}\right)^{1/2}\right]^{1/2} k_F. \tag{3.3}$$

Obviously, for thick tunneling barriers $k_\perp^{\max}/k_F$ is quite small, and one often assumes that $k_\perp^{\max} \simeq 0$.[15] However, for short coherence length superconductors with small k_F, and small barrier widths, such as in the case of soft-point-contact tunneling,[5] one can expect to have $k_\perp^{\max}$ of order $0.1\,k_F$, and hence our choice of $k_\perp^{\max}$. The probability p in (3.1), and therefore the range $k_\perp^{\max}$, in general, depends weakly on energy E, in the energy regime considered. The above argument does not apply to the cases in which particles tunnel through a sharp tip, where the local electric field is very strong. This is the case in most vacuum tunneling measurements. There the strong electric field produces a very narrow, well-collimated particle beam,[14] and $k_\perp^{\max}$ is very small.

Returning to Fig. 3, one can observe a structure, characterized by a set of peaks, which is due to quasiparticle reflections at the insulating barriers. The quasiparticles then interfere and the result is a resonance pattern in the DOS. The structure of the peaks is different in the two cases. In the "more localized" case (the solid line), the higher energy peaks become almost equally spaced, which can be expected, since the interference with quasiparticles tunneling through the barrier is almost negligible. The resonance pattern is almost solely due to the scattering of particles within a single S layer. In contrast, as clearly shown by the dashed line, as the barrier height is reduced, more quasiparticles from neighboring layers can penetrate and create the calculated interference pattern. This pattern is due to the scattering of quasiparticles at the neighboring S-I interface, and since the thickness of the I layer is much smaller than that of the S layer, the peak shifts are only minor. In addition, the peaks, for the same amount of transverse momentum $k_\perp$ included,

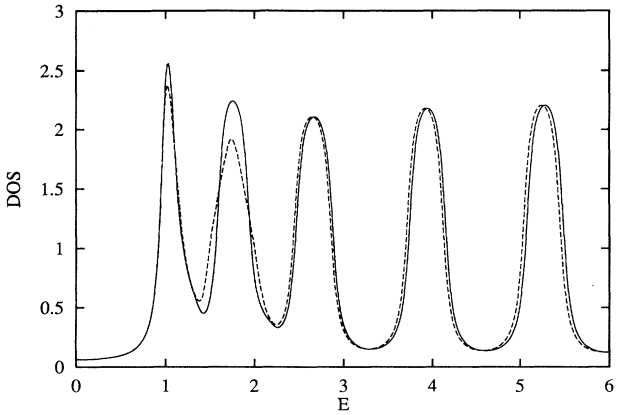

FIG. 4. As in Fig. 3, for the two systems depicted in Fig. 2. The solid and dashed lines here correspond to the systems displayed by the solid and dashed lines in Fig. 3, respectively.

are wider in the latter case, again consistent with lower barrier height.

On the other hand, if one compares the DOS for the two systems depicted in Fig. 2, which we do in Fig. 4, one finds that the interference pattern is almost unchanged. The solid (dashed) line here shows the system displayed by a solid (dashed) line in Fig. 2, and for the same value of $k_\perp^{\max}$ as in the previous figure. The peaks are almost in identical positions, especially for higher energies. Actually, what happens is that, although the barrier thickness is very small and therefore particles are allowed to tunnel and scatter (which can be best seen by looking at change in the shape of the second peak in the dashed line), the interference pattern shifts are determined by the ratio d_I/ξ_0, which is quite small in both cases, and therefore the two plots appear almost identical.

It is quite important to examine how the local DOS depends on the range of transverse momentum $k_\perp^{\max}$ included in the integration. The dashed line in Fig. 5 shows the DOS for the system depicted by the solid line in Fig. 1, with $k_\perp^{\max} = 0.1\,k_F$, while for comparison the solid line shows the same DOS as that shown by the solid line in Figs. 3 and 4. Two important differences are quite noticeable: First, the higher energy peaks in the dashed line are much broader, since the larger range of $k_\perp$ allows for an interference superposition for a larger energy range of quasiparticles. Second, at lower energies, we notice that an additional peak has emerged at $E \approx 2.1\,\Delta_0^S$. As previously mentioned, the observed peaks are the interference maxima and this new peak has to be attributed to the same phenomenon. We find that the new peak is in fact a "second harmonic" of the first one: By recalling the quasiparticle spectrum (2.9), it is obvious that the same band number ν with the same band vector k_z can produce superpositions at different energies with different amounts of transverse momentum included. This is significant in tunneling experiments on short coherence length materials, where a larger range of $k_\perp$ may come into play also because of surface scattering. Although this dependence may be less important in the vacuum tunneling case, where $k_\perp \to 0$, it is crucial in point-contact spectroscopy, where electrons with larger $k_\perp$ are included in the interference patterns. The strong dependence of the DOS on the $k_\perp$ range is largely due to the relatively small size of $k_F d_S$, and it is not observed in the case of less inhomogeneous materials, such as those studied in Ref. 3.

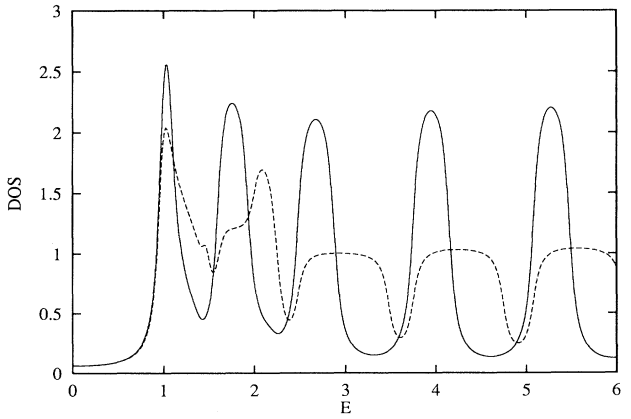

FIG. 5. Local DOS, normalized as in Fig. 2. Both curves correspond to the system depicted in Fig. 1. The solid line is obtained with $|k_\perp| = 0.04\,k_F$, and the dashed line with $|k_\perp| < 0.1\,k_F$.

In all of the previous plots we have assumed a short coherence length. In Fig. 6 we plot the DOS for the small $k_\perp^{\max} = 0.1 k_F$, and for the same thicknesses as the system depicted by the dashed line in Fig. 5, but this time for a longer $\pi k_F \xi_0 = 200$. Here the size of the S layer is smaller than the coherence length and therefore one must calculate the DOS by integrating Eq. (2.20) over the whole range of z up to d_S. As shown in Ref. 12, the OP will exhibit size effects. Thus, one should carefully compare plots for long and short ξ_0 materials. For long ξ_0 materials the ratio E_F/Δ_0^S is very large and therefore for the same amount of $k_\perp^{\max}$ the energy peaks are extremely broad. After averaging over an energy scale larger than Δ_0^S/E_F, as was done in previous work which included interference of quasiparticles,[15,16] one obtains the well-

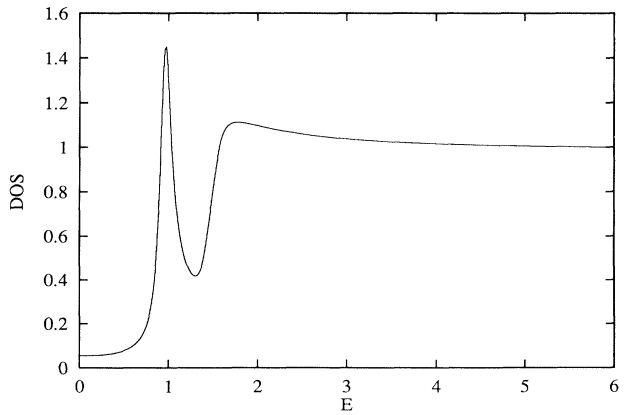

FIG. 6. Local DOS for a system with the same geometry and the barrier height as that shown in Fig. 1, but for a larger value of the coherence length $\pi k_F \xi_0 = 200$.

known square root singularity in the density of states. Note, however, that the same averaging is not justified when the coherence length is short in which case more detailed theories must be employed. For the intermediate ξ_0 value shown here some structure still remains at very low energies.

Finally, we turn to the most important question of comparison with experiments. Our results should be compared with experiments performed on those HTSC compounds which exhibit the largest amount of anisotropy, such as BSCCO. In particular, it is interesting to compare our results to the tunneling data obtained in point-contact experiments, where a larger amount of $k_\perp^{\max}$ should be present. Therefore we compare with the tunneling spectra[5] in BSCCO, recently obtained using a soft-point-contact STM spectroscopy.

The comparison with experiments involves several important considerations regarding the applicability of the theory and the input parameters. We discuss here most of these questions, particularly those that directly affect comparison with the data, and refer the reader to the next section for other related points. First, the crystal structure of BSCCO is nontrivial: Although its lattice constant in the c direction is approximately 30.8 Å, the unit cell of BSCCO can be viewed as consisting of two shifted subcells separated by insulating BiO layers, each having three copper-oxide planes, translated with respect to each other in the ab plane. Since we assume that the metallic part of each subcell is uniform in the x, y directions, which is adequate for the study of tunneling in the c direction, we have $d = 15.4$ Å. The insulating layer distance can be estimated from the distance between neighboring Bi atoms[17,18] as $d_{\mathrm{I}} \simeq 1.5$ Å. We must also include the large mass anisotropy of BSCCO: m_c/m_{ab} has been reported[19] to be anywhere between 60 and 250. However, the obtained results barely depend on m_c/m_{ab}, provided $m_c/m_{ab} \gg 1$. Therefore we assume $m_c/m_{ab} = 100$. In addition, in Ref. 5 it was estimated that the coherence length in the c direction, ξ_c, is of order 1.6–1.75 Å in BSCCO. In our calculations we assume $\xi_0 = 1.6$ Å. We obtain $k_F \approx 0.5$ Å^{-1} from the carrier density reported in Ref. 19. The formula $(m_c/m_{ab})^{1/2}\pi k_F \xi_0 = 2E_F/\Delta_0^S$ yields the ratio Δ_0^S/E_F, which is the input quantity in the calculation. A simultaneous change of the mass anisotropy ratio and the Fermi wave vector does not affect the computations as long as E_F/Δ_S^0 remains constant. As pointed out in connection with Fig. 3, the results for the DOS are not too sensitive to the choice of V_0 in the range considered. Thus, we have here fixed $V_0 = 1.5\,E_F$. The remaining parameter Δ_0^S/ω_0 is not known *a priori*. We determine its value as follows: We calculate the transition temperature T_c (in units of E_F) by solving Eqs. (2.16), (2.17), and (2.19) at increasing temperatures until that at which the OP vanishes is found. This is done, as a function of Δ_0^S/ω_0, and this way, knowing the experimentally observed $T_c \approx 90$ K, we establish the energy scale for our comparison of the DOS. The best agreement with the experimental energy scale is achieved by setting $\Delta_0^S/\omega_0 \approx 0.4$. This parameter, together with $k_F\xi_0$, is then used to determine $g(z)$. One can simply assume $g(z) = \text{const}$ in the S layer, but it is more realistic, for this compound, to assume $g(z) = g_1$ when z is in a region in the middle of the S layer, centered around the copper-oxide planes (where the coupling is believed to be stronger), and $g(z) = g_2 < g_1$ in the rest of the S layer. In our calculation we have fixed $g_2 = 0.5\,g_1$. However, provided that the input parameters remain the same, the DOS depends only very weakly on the specific form of $g(z)$ chosen, and there is only a slight shift in the first peak in the DOS.

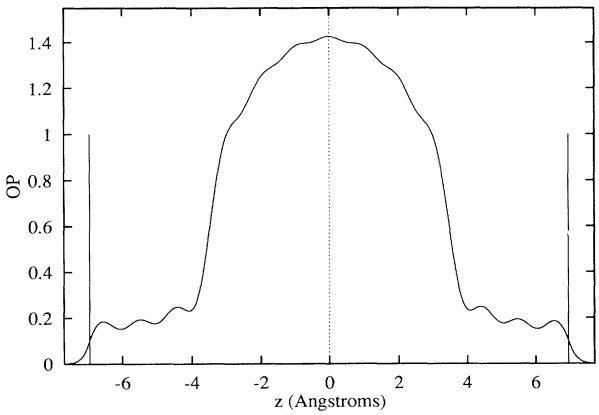

FIG. 7. Normalized OP $\Delta(z)/\Delta_0^S$, in our model of BSCCO (see text). The OP assumes larger value in the stronger coupling region of CuO planes, $d = 8$ Å, in the middle of the S layer. The vertical lines mark the insulating region.

We begin by presenting our results for the OP in the superconducting (metallic) layer, as shown in Fig. 7. It is clear that the OP reaches values on the order of Δ_0^S, in the region where the coupling is larger. Consistently with the findings of Ref. 3, the OP varies predominantly inside that region and only slightly elsewhere. As a consequence of the lower OP value in the weaker coupling region [$g(z) = g_2$], the OP extends into the I layer only marginally. The larger value of the OP inside of the stronger coupling region is in agreement with the common belief that the OP is very large only within the CuO planes, but can be very small elsewhere.

To calculate the experimentally measured DOS, we must still consider the appropriate value of $k_\perp^{\max}$, since, as shown in Fig. 5, the DOS results are quite sensitive to this value. This is nontrivial, since in the experiments $k_\perp^{\max}$ itself varies with the bias energy E, i.e., the energy of the probing particle. It follows from the discussion of Eqs. (3.1)–(3.3) that this variation is approximately linear in E for $k_\perp$ small. Therefore, we have chosen $k_\perp^{\max} = k_F\,(0.04 + 0.1\,E/E_F)$. Here the coefficients may be viewed as adjustable parameters, which control the width and height, but not the position, of the DOS peaks (see Fig. 5).

Figure 8 shows the fit of our results (solid line) to the experimental data (dashed line) of Ref. 5: The energy is in the same units of voltage as in the experiment, and the DOS is scaled with respect to its normal-metal limit. The theoretical curve is shifted by –0.4 for clarity. The linear background of the experimental data has been included in a similar manner as in Ref. 5, and the theoretical result is convolved with a Gaussian of width 10 meV, in

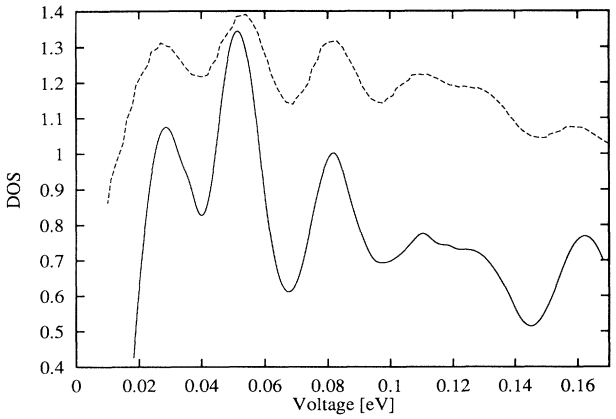

FIG. 8. Comparison of the theoretical results (solid line) for the DOS (see text) with the tunneling spectra of BSCCO (dashed line). The theoretical curve has been shifted vertically by -0.4 for clarity. Here $|k_\perp| < k_F\,(0.04 + 0.1\,E/E_F)$.

order to account for the finite energy widths found in the experiment. Obviously the agreement is quite good, and in fact significantly better than that obtained in Ref. 5, where a non-self-consistent approach was employed. The fit could be further improved by a more detailed study of the $k_\perp^{\max}$ dependence, surface roughness, or the impurity scattering in the experiment. A more detailed knowledge of the experimental setup might remove all fitting parameters from our model. What is remarkable is that the peak positions and their rather intricate shape are matched almost perfectly, indicating that our model can account quantitatively for the experimental data (even if there are fitting parameters in the integration over $k_\perp$). This was not possible using non-self-consistent theories,[5] since only a self-consistent calculation could produce the relatively large "energy gap" values (located by the position of the first peak), seen in the actual experiment, and due to the fact that the OP never goes to zero in the superconducting layer. Just as in Refs. 3 and 20, the "energy gap" is not equal to the maximum value of the OP in the S layer. The most important difference, however, comes from the fact that the pattern is due to resonant scattering on the insulating layers, rather than on the S-N interfaces. Moreover, in Ref. 5 it was found that the DOS pattern may vary in different experimental situations, and from our study it follows that the difference should be attributed to a variation of $k_\perp^{\max}$ and the energy resolution, rather than to whether the outermost layer is a superconducting or a normal-metal one.

IV. CONCLUSIONS

In this paper we have performed a study of superconductor-insulator inhomogeneous superconducting structures, using a microscopic method based on the Gor'kov equations. We have expanded these equations in terms of appropriately chosen Bloch functions in the tight-binding approximation. The equations then transform into a set of matrix equations which we solve self-consistently to obtain the order parameter (pair potential) and the tunneling density of states.

In the study of the experimentally relevant situations where the size of the insulating barrier is small, we find that the minimum OP value in an I layer is very low, provided that the barrier height is sufficiently above the Fermi energy. This justifies the use of the tight-binding approximation for this system. We find that this method is correct even when the barrier is relatively thin. On the other hand, the local DOS is a stronger function of the barrier width in that the observed peaks are somewhat shifted. We also find that the calculated DOS depends significantly on the range of $k_\perp$ included in the calculation, than in the SN multilayer case studied in Ref. 3, for the thickness ranges considered. The consequence is that, since the $k_\perp$ range varies with a particular experimental situation, similar experiments may produce different results, depending on the sample quality or the experimental setup.

When comparing to experiments, we find that the calculated DOS agrees very well with the spectra obtained in a soft-point-contact STM tunneling measurement. Therefore, our conclusion is that the interference pattern, seen in the experiment, is due to the presence of insulating layers, and that the different patterns observed at different positions of the same crystal can in fact be explained by the above mentioned variation of the $k_\perp$ range involved, certainly present in point-contact experiments. Of course, comparison of theoretical results with a single experiment, no matter how successful, cannot be viewed as conclusive proof of the soundness of the applicability of the theory to that specific experimental situation, particularly when the comparison involves a number of assumptions for the input parameters. Nevertheless, our results strongly suggest that the presence of the finite thickness insulating layers should be seriously taken into account in tunneling experiments on BSCCO compounds.

The limitations present in this theory are as in previous work:[3,12] Since we are dealing with short ξ_0 materials, the superconducting coupling may be large, and one should consider a strong-coupling formalism.[21] One might even object to the representation of the insulating layers as an "external" potential in the Gor'kov equations on the grounds that this should be done only when the spatial variation of $U(z)$ and other quantities is slow, compared to interatomic distances. However, our use of $U(z)$ is not less justified than that of pseudopotentials in band structure calculations. In addition, we have excluded the experimentally confirmed ab-plane anisotropy,[22] but this is only a minor qualm, since this anisotropy should only marginally affect the c-axis tunneling discussed here. We have used a conventional s-wave pairing state, which may not be correct for high-temperature superconductors of the BSCCO class, as suggested by angle-resolved photoemission spectroscopy.[23] Moreover, the temperature and the impurity concentration dependence of the results may be nontrivial. Nevertheless, the conclusions regarding geometric resonances in the DOS should remain approximately the same in any system with a similar energy spectrum, with only possibly shifts in the size and positions of the peaks.

ACKNOWLEDGMENTS

We thank the Minnesota Supercomputer Institute for a grant of computer time. We have benefited from fruitful conversations with C. E. Campbell, M. G. Friesen, A. M. Goldman, R. A. Klemm, J.-X. Liu, and S. W. Pierson. We are indebted to G. Spalding for many useful discussions and for reading an early version of this manuscript. One of us (B.P.S.) gratefully acknowledges the support of the U.S. Department of Education.

---

* Present address: Department of Physics and Materials Research Laboratory, University of Illinois, Urbana, IL 61801.

[1] See, e.g., P. Monthoux and D. Pines, Phys. Rev. B **49**, 4261 (1994).

[2] See, e.g., S. H. Liu and R. A. Klemm, Phys. Rev. B **45**, 415 (1992); A. A. Abrikosov, Physica C **182**, 191 (1991).

[3] B. P. Stojković and O. T. Valls, Phys. Rev. B **50**, 3374 (1994).

[4] R. Kleiner, F. Steinmeyer, G. Kunkel, and P. Müller, Phys. Rev. Lett. **68**, 2394 (1992); R. Kleiner and P. Müller, Phys. Rev. B **49**, 1327 (1993).

[5] J.-X. Liu, S. W. Pierson, G. C. Spalding, J.-C. Wan, and A. M. Goldman, Europhys. Lett. **20**, 721 (1992).

[6] W. E. Lawrence and S. Doniach, in *Proceedings of the International Conference on Low Temperature Physics,* Kyoto, 1970, edited by E. Kanda (Keigaku, Tokyo, 1971), p. 361.

[7] For compounds such as BSCCO, the coherence length in the c-crystallographic-axis direction, ξ_c, is shorter than the unit cell. See, e.g., R. J. Donelly, in *A Physicist Desk Reference*, edited by Herbert L. Anderson (American Institute of Physics, New York, 1989).

[8] M. Tachiki and S. Takahashi, Physica C **191**, 363 (1992).

[9] See, e.g., D. A. Wollman, D. J. Van Harlingen, W. C. Lee, D. M. Ginsberg, and A. J. Leggett, Phys. Rev. Lett. **71**, 2134 (1993); P. Chaudhari and Shawn-Yu Lin, *ibid.* **72**, 1084 (1994).

[10] A. A. Abrikosov, L. P. Gor'kov, and I. E. Dzyaloshinski, *Methods of Quantum Field Theory in Statistical Physics* (Prentice-Hall, Englewood Cliffs, NJ, 1963).

[11] Branko P. Stojković and Oriol T. Valls, Phys. Rev. B **47**, 5922 (1993).

[12] Branko P. Stojković and Oriol T. Valls, Phys. Rev. B **49**, 3413 (1994).

[13] T. Giamarchi, M. T. Béal-Monod, and O. T. Valls, Phys. Rev. B **41**, 11 033 (1990).

[14] Gabriel Spalding (private communication).

[15] O. Entin-Wohlman and J. Bar-Sagi, Phys. Rev. B **18**, 3174 (1978).

[16] W. J. Gallagher, Phys. Rev. B **22**, 1233 (1980).

[17] J. C. Phillips, *Physics of High-T_c Superconductors* (Academic Press, San Diego, 1989).

[18] J.-X. Liu, J.-C. Wan, A. M. Goldman, Y. C. Chang, and P. Z. Jiang, Phys. Rev. Lett. **67**, 2195 (1991).

[19] D. R. Harschman and A. P. Mills, Jr., Phys. Rev. B **45**, 10684 (1992), and references therein.

[20] S. H. Liu and R. A. Klemm, Phys. Rev. Lett. **73**, 1019 (1994).

[21] G. M. Eliashberg, Zh. Eksp. Teor. Fiz. **38**, 966 (1960) [Sov. Phys. JETP **11**, 696 (1960)].

[22] For a review on the *ab*-plane anisotropy see, e.g., *Physical Properties of High Temperature Superconductors*, edited by D. M. Ginsberg (World Scientific, Singapore, 1992), Vol. III.

[23] Z.-X. Shen, D. S. Dessau, B. O. Wells, D. M. King, W. E. Spicer, A. J. Arko, D. Marshall, L. W. Lombardo, A. Kapitulnik, P. Dickinson, S. Doniach, J. diCarlo, A. G. Loeser, and H. C. Park, Phys. Rev. Lett. **70**, 1553 (1993).